Study on Morphology and Microstructure Development of PA6/LDPE/Organoclay Nanocomposites

Vahid Khoshkava, Maryam Dini, Hossein Nazockdast

Polymer Engineering Department, AmirKabir University of Technology, Tehran, Iran

Received 21 July 2010; accepted 15 December 2010
DOI 10.1002/app.33970
Published online 31 December 2011 in Wiley Online Library (wileyonlinelibrary.com).

ABSTRACT: The aim of this work was to study the morphology and microstructure development of the polymer blend nanocomposite samples. The samples were prepared by melt compounding, consisting of the melt intercalation and melt blending processes, in an internal mixer at temperature of 250°C. The XRD characteristic peaks of the organoclay were almost disappeared in the polyamide (PA6)/Organoclay and PA6/low density polyethylene (LDPE)/organoclay samples. The TEM results revealed a partially exfoliated type microstructure in which the tactoids and/or platelets were finely dispersed in PA6 matrix. The results of the melt linear viscoelastic measurements showed that most of the organoclay in PA6/LDPE/Organoclay were preferentially dispersed in PA6 matrix. The scanning electron microscopy results showed nonterminal low frequency behavior in storage modulus indicating much smaller LDPE particle size in the PA6/PE (85/15) nanocomposite samples compared to that in the simple blend. This could mainly be attributed to the hindrance induced reduction of the coalesance, the interfacial enhancement, and thermodynamic compatibility all caused by high aspect ratio organoclay platelets. The PA6/LDPE/organoclay samples exhibited a pronounced viscosity upturn and nonterminal storage modulus (G') with even greater extent than those observed for PA6/organoclay samples. These results were considered as indications that the presence of LDPE dispersed phase can have an enhancing effect on development of three-dimensional network structure in the polymer blend nanocomposite samples. © 2011 Wiley Periodicals, Inc. J Appl Polym Sci 125: E197–E203, 2012

Key words: nanocomposite; melt linear viscoelastic; microstructure

INTRODUCTION

Blending of two or more different polymers has proved to be one of the most successful methods for developing new materials with desirable properties.[1,2] The main reasons of blending polyolefins with polyamides are either to improve particular properties of the polyamides, such as toughness, moisture absorption, or process ability, or to promote the performance of the polyolefins with respect to properties such as rigidity, thermal stability, and barrier properties to oxygen and solvents.[3]

Recent studies have shown that fillers can even alter the phase stability and the morphology of polymer blends as a result of a strong adsorption of polymeric components on the solid surface.[4] To achieve this function, the inorganic components should have the largest possible surface area per unit weight such as: layered silicates, calcium carbonates, and other nanoparticles. During the last two decades, numerous researches have been devoted to polymer-layered silicate nanocomposites due to their attractive technological applications and scientific issues.[5–7] Many of these research works have been focused on nanocomposite based on polyamide,[8–10] polyimide,[11] polystyrene (PS),[12] and polyolefin.[13]

In recent years, there has been a growing interest in the polymer blend nanocomposites due to their enhanced physical and mechanical properties.[14–17] It has been shown that the presence of organoclay in the polymer blend nanocomposites in addition to enhancing effect can also act as compatibilizing agent.[18–22] Although the mechanisms of compatibilization are still not clear, it has been accepted that the presence of nanofillers can affect the morphology of the polymer blends. Gelfer found that the PS domain size in PS/polymethyl methacrylate blend was reduced on adding organoclays and increased viscosity.[20] Also, Wang et al. showed that in PS/PP system, PS particle size is greatly decreased on the addition of organoclay. They suggested that immiscible polymer chains can exist together between the intercalated clay platelets and play the role of a block copolymer.[21] It has been shown that depending on the interaction of clay with the blend components, three possible partitioning can exist for nanoclay; clay is preferentially located in one phase, dispersed in both blend components polymers, and located at the interface.

Correspondence to: H. Nazockdast (nazdast@aut.ac.ir).

Compositions of Prepared Samples in Internal Batch Mixer

Sample	PA6 (wt %)	LDPE (wt %)	Organocaly (phr)
Ln2	0	100	2
Pn2.3	100	0	2.3
P85L15	85	15	0
P85L15n0.5	85	15	0.5
P85(Ln5)[a]	85	15	0.5
P85L15n1	85	15	1
P85L15n2	85	15	2
P85(Ln11)[a]	85	15	2
P85L15n4	85	15	4
P70L30	70	30	0
P70L30n1.6	70	30	1.6

[a] Prepared in different order feeding, that is, first preparation of nanocomposite-based LDPE then mixed it with PA6 as a dispersed phase.

It has been shown that melt-rheological study of polymer-layered silicate nanocomposites can provide great insight into understanding polymer–filler interactions and microstructure development of nanocomposites. This is because material-rheological functions are strongly influenced by the structure and the interfacial properties.[23–27]

polyamide (PA6)/low density polyethylene (LDPE) is widely used in film and injection applications. However, adding LDPE leads to a lower strength of PA6. As morphology and final properties of a blend are correlated, in this study the effect of organoclay on development of morphology for a blend of PA6/LDPE was investigated.

EXPERIMENTAL

Materials

A commercial PA6 [Akulon (F133-c2)] with melt flow index 14 g/10 min (MFI at 240°C and 2.16 kg loads) was used as a matrix. A LDPE (LF0200) with MFI 2g/10 min (190°C and 2.16 kg loads) was used as minor component of the blends purchased by BIPC (Bandar Imam Petrochemical).

Two different organically modified layered silicates used in this Study were Cloisite®30B (C30B) and Cloisite® 15A (C15A), both supplied by Southern Clay products (Gonzalez, TX, USA). C30B and C15A are natural montmorillonite modified with methyl, tallow, is-2-hydroxyethyl, quaternary ammonium (Mt2ETOH) and dimethyl, dehydrogenated tallow, quaternary ammonium (2M2HT), respectively. The cation exchange capacity of C30B was 90 mequiv/100 g and that of C15A 125 mequiv/100 g.

Melt blending

Polymer blend nanocomposite samples varying in composition as listed in Table I were investigated. All the samples were prepared in a laboratory internal batch mixer (Brabender®, Duisburg, Germany) at temperature 250°C and rotor speed 60 rpm. All samples, otherwise specified, were prepared by direct feeding of the organoclay into the PA6/LDPE blend in an internal mixer.

Characterization

The morphology of the blend samples were studied by using scanning electron microscopy (SEM; Philips XL30 model, apparatus operating at an accelerating voltage of 20 kv). The cryogenically fractured surface of the samples was sputtered with gold to avoid charging. The XRD patterns of the samples were recorded on a Rigaku X-ray diffractrometer with nickel filtered Cu-K_α _ radiation ($\lambda = 0.154$ nm)operated at 50 Kv and 150 Ma. Data were obtained over the range $2\theta = 1.5°$ to 10°. The melt linear viscoelastic properties of the samples were studied using a rheometric mechanical spectrometer (Paar Physica USD200), with a parallel plate (diameter = 2.5 cm; gap = 1 mm) geometry at 240°C and at strain of 1% to ensure the linear viscoelastic region.

RESULTS AND DISCUSSION

XRD results

Figure 1 shows the XRD patterns of the neat organoclays, PA6/organoclay and LDPE/organoclay nanocomposite samples. The XRD pattern of organoclay (30B) shows a broad single peak at around $2\theta = 4.73$, corresponding to a basal spacing of 1.86 nm. As it can be noticed for PA6/clay nanocomposites, the characteristic peak of the organoclay is almost disappeared. These results indicate that a highly intercalated or partially exfoliated microstructure was developed in PA6/organoclay nanocomposite, which originates from the hydrophilic nature of C30B, which is in agreement with literature.[28]

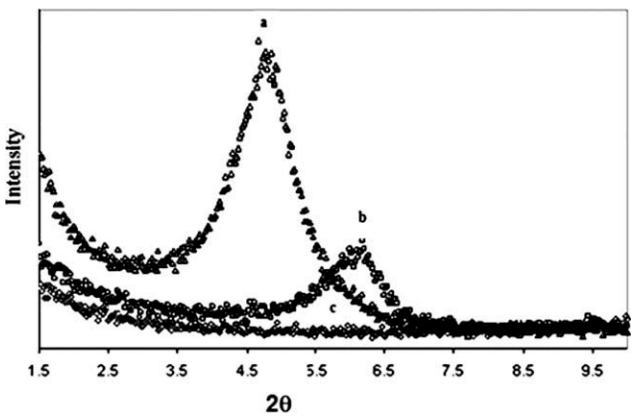

Figure 1 XRD patterns of (a) organoclay powder, (b) Ln4, and (c) Pn2.3.

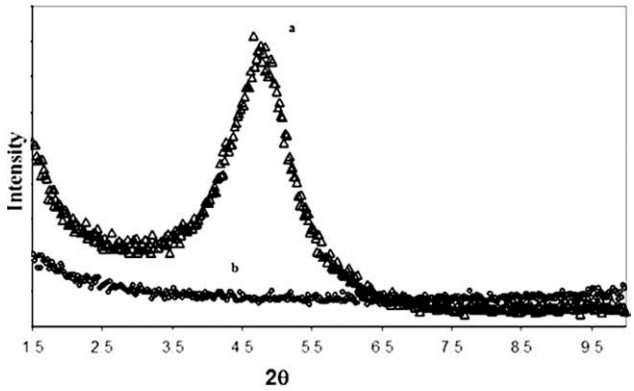

Figure 2 XRD patterns of (a) Organoclay powder and (b) P85L15n2.

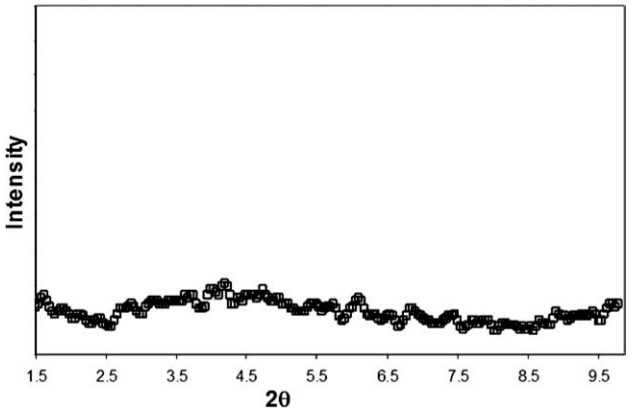

Figure 3 XRD pattern of L85L15Pn2.

Figure 1 also shows that PE matrix in the absence of compatibilizer is not capable of intercalating the organoclay stacks. The additional peak observed in LDPE/organoclay sample, the characteristic peak of the organoclay was shifted to greater 2 indicating that for this sample the gallery distance of the organoclay was decreased. This can be attributed to degradation of the intercalants in the high temperature (250°C) of the processing.[29] The result of the PA6/LDPE/organoclay hybrid sample is shown in Figure 2. As seen in the figure,there is no characteristic peak of organoclay, and this may refer to the organoclay affinity into PA6 phase. To justify this, we examined the morphology of another sample when was prepared by using different feeding order. Figure 3 shows the XRD pattern of a PA6/LDPE/organoclay sample, which was prepared by first melt mixing of LDPE with organoclay and the melt compounded with PA6. Abbreviation L85P15n2 has been used for this sample. Comparing this result with those shown in Figure 2, one may notice that affinity of organoclay with PA6 is strong enough for migration of the organoclay from LDPE phase into the PA6 matrix. In other words, it is indicating that the organoclay (C30B) has a greater affinity toward PA6.

TEM results

Figure 4 shows the TEM micrograph of the PA6/Organoclay nanocomposite sample. These results indicate that a highly intercalated or partially exfoliated type microstructure is formed in which the organoclay platelates and/or tactoids are finely dispersed in PA6 matrix.

Morphology

Figure 5 shows the SEM micrographs of the PA6/LDPE samples with the same blend ratio (85/15 w/w) but varying in organoclay content (0, 1, 2, and 4 phr). By comparing these results one can clearly

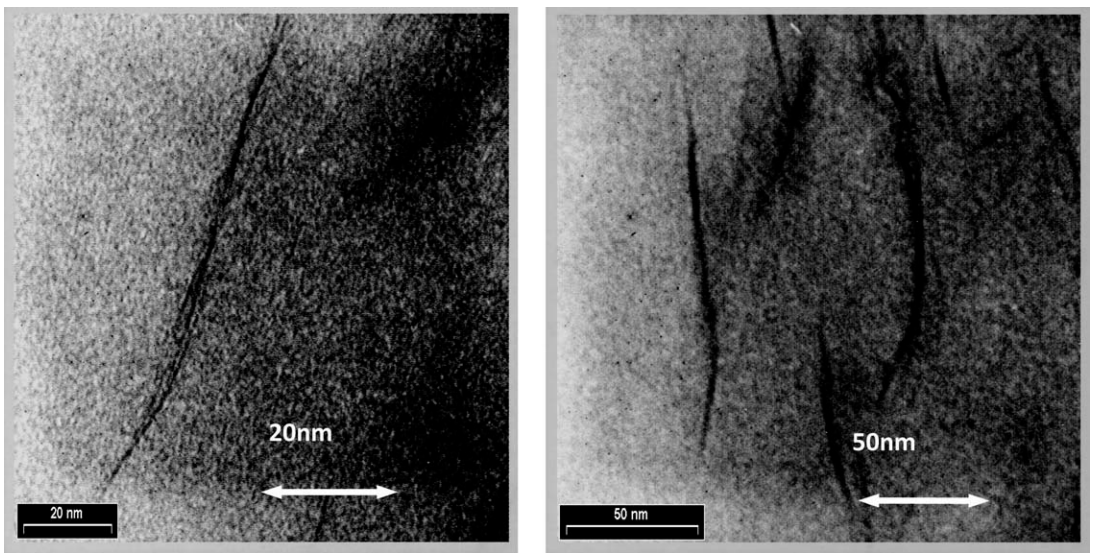

Figure 4 TEM micrograph of nanocomposite-based PA6/organoclay.

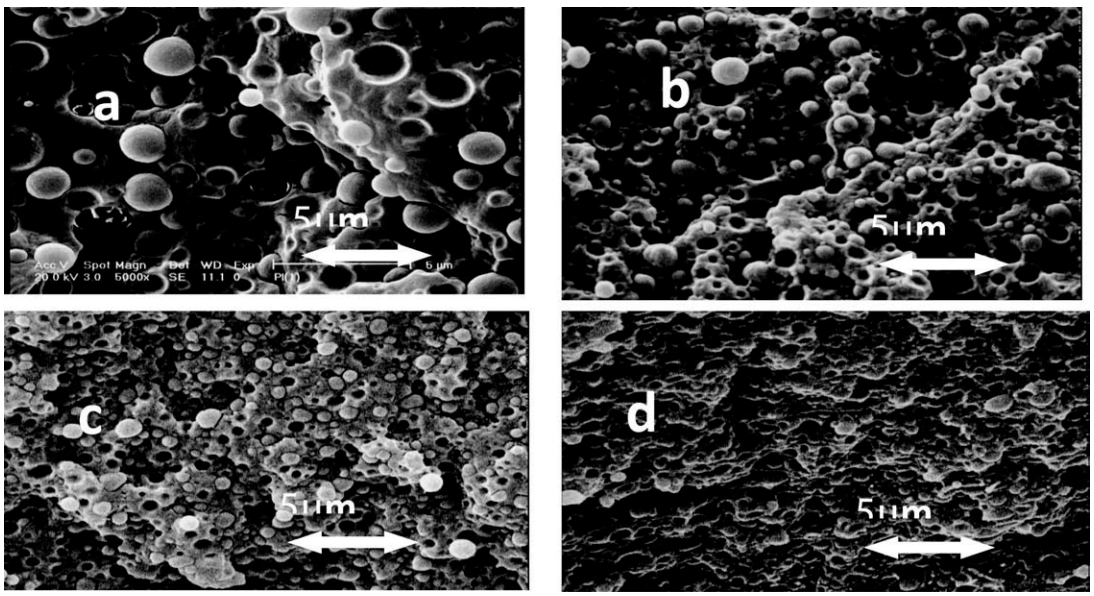

Figure 5 SEM micrographs of PA/LD (85/15 w/w) blend with (a) 0% (b) 1 wt %, (c) 2 wt %, and (d) 4 wt %.

notice that the LDPE particle size in the polymer blend nanocomposite samples is much smaller than that in the simple blend. Moreover, the LDPE particle size decreased with increasing organoclay concentration. This could be attributed to intensify the coalescence reducing effect on droplet size caused by high aspect ratio organoclay platelets in PA6 matrix. The hindrance induced reduction of coalescence caused by organoclay platelets has been reported by other researchers.[18–22] The reduction of interfacial tension, caused by presence of organoclay in the interphase, can also play a role. To clarify this, another nanocomposite blend sample with the same composition but prepared with using different feeding order (two-step feeding order) was considered. This sample was prepared by first melt mixing the LDPE with 0.5 phr organoclay, and the resulting mixture was melt blended with PA6 in the later stage of mixing. Figure 6 compares the SEM micrograph of these two samples. As it can be seen from Figure 6, the LDPE particle size in the sample prepared by using two-step methods is much smaller than that in the one-step feeding prepared sample. As the organoclay platelets has a greater affinity to the PA6 matrix phase, they can easily migrate from LDPE phase, and during this process, a fraction of organoclay may trap in the interphase and cause the reduction of the LDPE particle size by enhancing the interfacial interaction. Increasing the polarity of the nonpolar LDPE phase by first adding organoclay may also play a role in increasing the compatibility and therefore reducing the LDPE particle size.

The SEM micrographs of PA6/LDPE simple blend with blend ratio of 70/30 w/w shown in Figure 7 suggest a semicocontinuous type morphology,

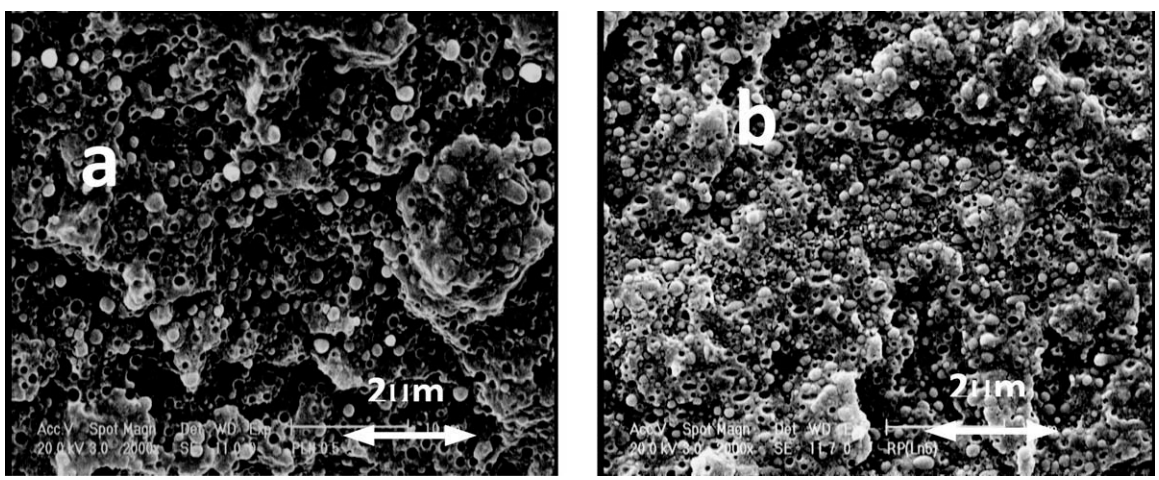

Figure 6 SEM micrograph of (a) P85L15n0.5 and (b) P85 (Ln5).

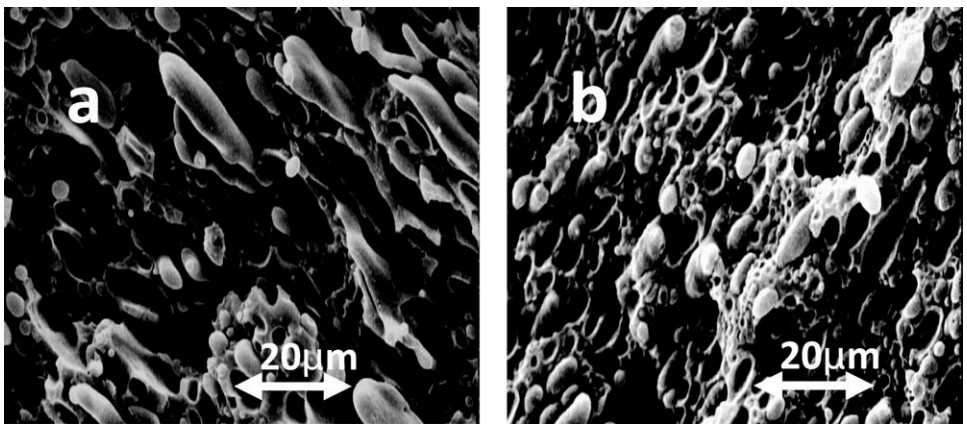

Figure 7 SEM micrographs of PA/LD (70/30 w/w) blend with (a) 0 phr organoclay and (b) 2 phr organoclay.

whereas the PA6/LDPE (70/30 w/w) blend sample containing 2-phr organoclay shows a matrix-dispersed morphology [Fig. 7(b)]. These results suggest that the presence of organoclay platelets in PA6 phase hinders the coalescence of LDPE droplets to form a continuous phase and/or stabilize the PE droplet by decreasing the interfacial tension between PA6 matrix and LDPE dispersed phase.

Rheological results

Figure 8 shows storage modulus (G') as a function of frequency for LDPE, PA6, and PA6/LDPE (85/15 w/w) simple blend sample. These results indicate that LDPE is more pseudo plastic and exhibits greater melt elasticity at low shear rates compared with PA6. Similar experimental results obtained for the polymer blend nanocomposite samples with the same blend ratio (85/15 w/w) but varying in organoclay content are shown in Figure 9. As it can be noticed the polymer blend nanocomposite samples containing more than 2 phr organoclay exhibit a low frequency nonterminal behavior in storage modulus whose plateau magnitude increases with increasing organoclay content. These results indicate that organoclay is selectively intercalated or partially exfoliated in PA6 matrix.

Figure 10 compares storage modulusversus frequency of PA6-based nanocomposite sample containing 3.4 and 6 phr organoclay with polymer blend samples with 2 and 4 phr organoclay.

These results reveal that the low frequency storage modulus value of the polymer blend nanocomposite samples are much greater than those of PA6-based nanocomposite samples containing even higher organoclay content. This can be explained in terms of additional melt elasticity caused by PE droplet deformation enhanced interfacial and /or the new network formed between organoclay platelets in the presence of LDPE.

However, if we consider the total low frequency storage modulus, G'_{total}, of nanocomposite blend sample to be sum of storage modulus of PA6-based nanocomposite, 0.85×146 Pa $= 124.1$ Pa, and the elastic response of LDPE droplet, $0.15 \times 339 = 50.85$

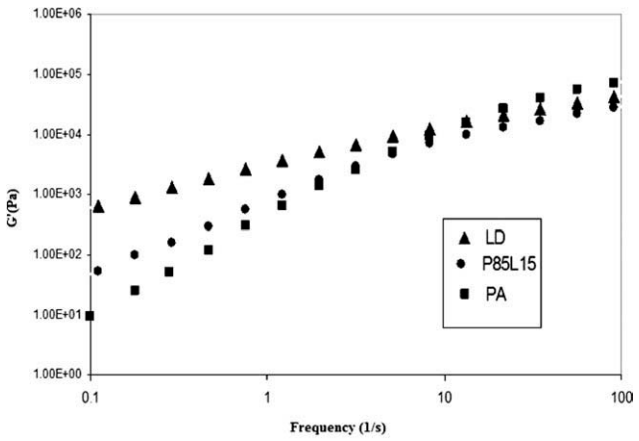

Figure 8 Storage modulus (G') versus frequency at 240°C for LD, PA6, and P85LI5.

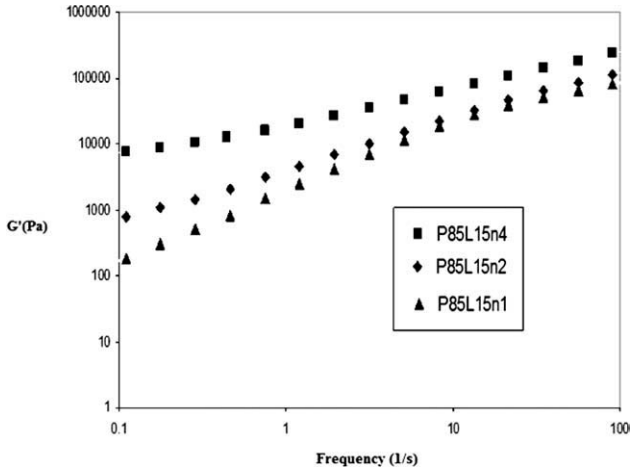

Figure 9 Storage modulus (G') versus frequency at 240°C for P85LI5n4, P85LI5n2, and P85LI5n1.

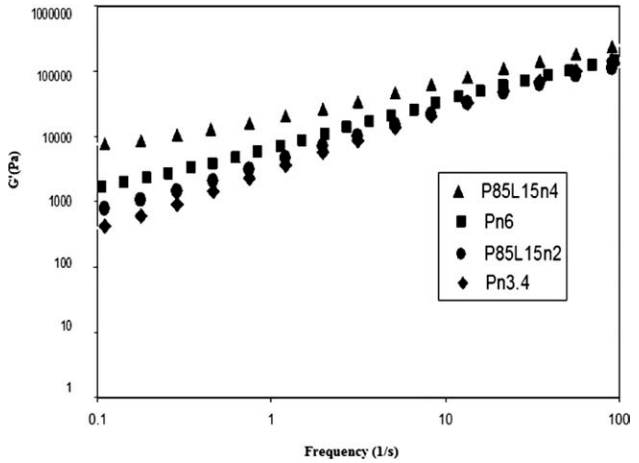

Figure 10 Storage modulus (G') versus frequency at 240°C for P85LI5n4, Pn6, P85LI5n2, and Pn3.4.

Pa, and the storage modulus due to interfacial interaction between two phases, $3 \times 36.7 = 101.1$ Pa, (multiply by three as a result of reducing LDPE droplet size) estimated from the simple blend then the results will be 258 Pa, which is much lower than the value of storage modulus found from experimental results 792 Pa. Therefore, there must be another reason behind the strong increase in storage modulus of the nanocomposite blend sample.

These results suggest that the presence of LDPE droplet in PA6 matrix containing organoclay with an almost exfoliated microstructure can rearrange the tactoid or platelets leading to a new network microstructure with stronger strength than that formed by interconnecting platelets themselves. Moreover, as it can be seen in Figure 11, the steady state torque of PA6/LDPE (85/15 w/w) blend sample shows a pronounced increase as the organoclay is added into the molten mixture, whereas in the case of PA6/organoclay sample, the steady state torque almost remains unchanged (arrows in Fig. 11 indicate the time of adding organoclay). Considering the extent

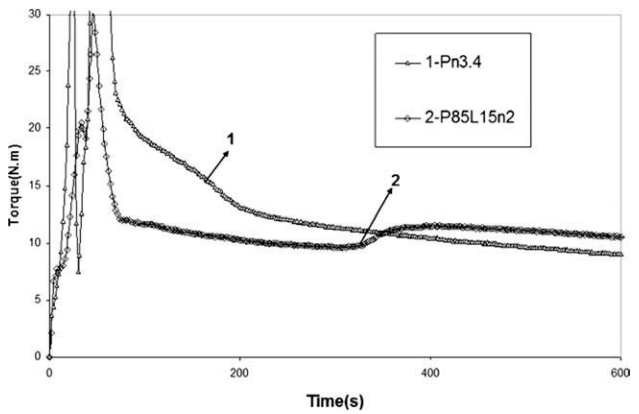

Figure 11 Torque-time graph of at 250°C and rotor speed 60 rpm.

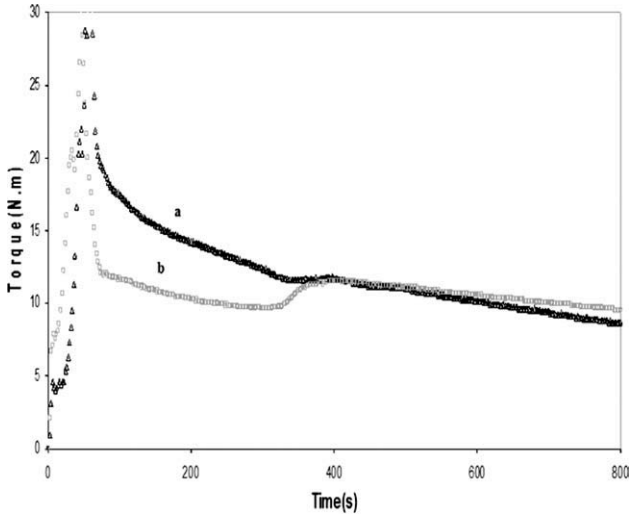

Figure 12 Torque-time graph of polymer nanocomposite containing 2 phr organoclay at rotor speed 60 rpm (a) and 120 rpm (b).

of deformation rate imposed on the mixture in the internal mixer, which is about $90s^{-1}$, such increase in the torque could hardly be due to the network form between tactoids.

Figure 12 compares the mixing torque versus time obtained for polymer blend nanocomposite samples prepared at two different rotor speeds of 60 and 120 rpm. As it can be noticed, there is no sign of sudden increase in mixing torque of the blend nanocomposite sample as a result of feeding organoclay. This reveals that the extent of imposed deformation (rotor speed 120 rpm) is high enough to break down the stronger network formed in this sample.

It should be noted that the above observed increase in the mixing torque did not occur in the polymer blend nanocomposite sample containing

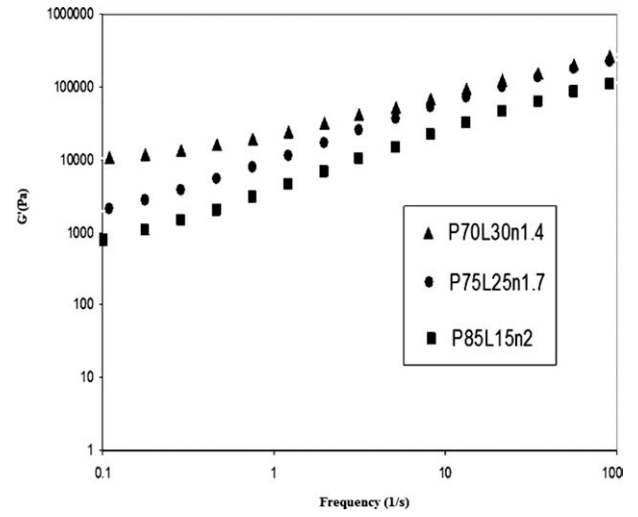

Figure 13 Storage modulus (G') versus frequency at 240°C for P70L30n1.4, P75L25n1.7, and P85L15n2.

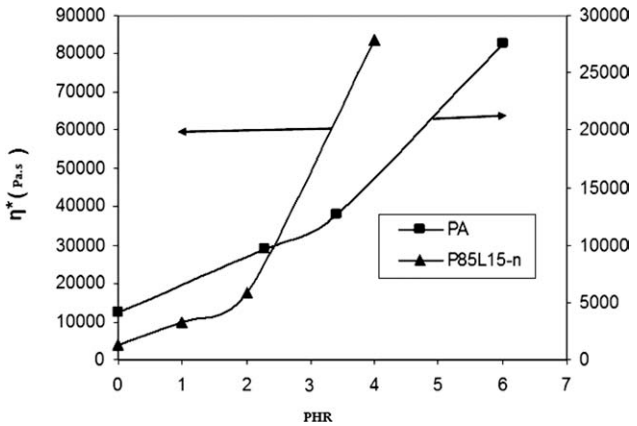

Figure 14 Complex viscosity as a function of organoclay concentration at $\omega = 0.1\ s^{-1}$.

cloisite15A. This suggests that effectiveness of PE droplets on the formation and strength of three-dimensional (3D) physical structure depend on the extent of exfoliation formed in PA6 matrix.

The effect of LDPE content on viscoelastic behavior of the simple blend samples and nanocomposite sample containing the same organoclay content are shown in Figure 13. By comparing these results, one may find out that the presence of LDPE in hybrid samples plays more effective role enhancing low frequency storage modulus of the hybrid sample.

Further evidences can be obtained from the results shown in Figure 14, which compares the complex viscosity at frequency $0.1\ s^{-1}$ versus organoclay content of PA6/organoclay nanocomposite and PA6/LDPE (85/15 w/w) nanocomposite hybrid sample. As it can be noticed, the results of viscosity versus organoclay concentration exhibit a percolation threshold whose value is higher for PA6 nanocomposite sample than that in PA6/LDPE blend nanocomposite sample.

CONCLUSIONS

It was shown that in PA6/LDPE/organoclay system due to greater affinity of polar organoclay (C30B) with PA6 the melt intercalation selectively occurred in PA6 phase.

From SEM results, it was found that LDPE particle size in PA6/LDPE/organoclay nanocomposite samples was smaller than that in PA6/LDPE simple blend. This could be explained in terms of reduction of PE droplet coalescence, interfacial interaction enhancement, and thermodynamic compatibility between the blend component all caused by highly aspect ratio organoclay platelets. The feeding order was found to have an influential effect on the LDPE particle in the blend nanocomposite sample. A pronounced low frequency nonterminal behavior of storage modulus exhibited by the nanocomposite samples was considered by an indication that organoclay is selectivity intercalated and partially exfoliated in PA6 in the form of 3D network. The low frequency storage modulus values of the polymer blend nanocomposite samples were found to be much greater than those of PA6-based nanocomposite samples containing even higher organoclay content. This was attributed to the presence of LDPE, which could rearrange the tactoids or platelets in the PA6 matrix leading to a new stronger network microstructure whose strength was highly depended on LDPE content and the organoclay concentration.

References

1. Huneault, M. A.; Shi, Z. H.; Utracki, L. A. Polym Eng Sci 1995, 35, 115.
2. Paul, D. R. Polymer Blends; Wiley, New York, NY, USA, 1999.
3. Holsti-Miettinen, R. M.; Perttilä, K. P.; Seppälä, J. V.; Heino, M. T. J Appl Polym Sci 1995, 58, 1551.
4. Lipatov, Y. S.; Nesterov, A. E.; Ignatova, T. D.; Nesterov, D. A. Polymer 2002, 43, 875.
5. Klein, J.; Kamiyama, Y.; Yoshizawa, H.; Israelachvili, Jacob N.; Fredrickson, Glenn H.; Pincus, P.; Fetters, v. Macromolecules 1993, 26, 5552.
6. Giannelis, E. P. Adv Mater 1996, 8, 29.
7. LeBaron, P. C.; Wang, Z.; Pinnavaia, T. J. Appl Clay Sci 1999, 15, 11.
8. Usuki, A.; Koiwai, A.; Kojima, Y.; Kawasumi, M.; Okada, A.; Kurauchi, T.; Kamigaito, O. J Appl Polym Sci 1995, 55, 119.
9. Yano, K.; Usuki, A.; Okada, A. J Polym Sci Part A: Polym Chem 1997, 35, 2289.
10. Vaia, R. A.; Jandt, Klaus D.; Kramer, Edward J.; Giannelis, Emmanuel P. Macromolecules 1995, 28, 8080.
11. Fornes, T. D., et al. Polymer 2002, 43, 2121.
12. Hasegawa, N.; Okamoto, H.; Hawasumi, M.; Usuki, A.; Appl Polym Sci 1999, 74, 3359.
13. Kawasumi, M.; Hasegawa, N.; Kato, K.; Usuki, A.; Okada, A. Macromolecules 1997, 30, 6333.
14. González, I.; Eguiazábal, J. I.; Nazábal, J. Eur Polym J 2006, 42, 2905.
15. Ahn, Y.-C.; Paul, D. R. Polymer 2006, 47, 2830.
16. Chow, W. S.; Mohd Ishak, Z. A.; Karger-Kocsis, J.; Apostolov, A. A.; Ishiaku, U. S.; Polymer 2003, 44, 7427.
17. Gahleitner, M.; Kretzschmar, B.; Pospiech, B.; Ingolic, E.; Reichelt N.; Bernreitner, K. J Appl Polym Sci 2006, 100, 283.
18. Wang, K.; Zhou, C. Polym Eng Sci 2001, 41, 2249.
19. Voulgaris, D.; Petridis, D. Polymer 2002, 43, 2213.
20. Gelfer, M. Y.; Song, Hyun H.; Liu, L.; Hsiao, Benjamin S.; Chu, B.; Rafailovich, M.; Si, M.; Zaitsev, V. J Polym Sci Part B: Polym Phys 2003, 41, 44.
21. Wang, Y.; Zhang, Q.; Fu, Q. Macromol Rapid Commun 2003, 24, 231.
22. Tang, Y.; Hu, Y.; Zhang, R.; Gui, Z.; Wang, Z.; Chen, Z.; Fan, Z. Polymer 2004, 45, 5317.
23. Ren, J.; Silva, A. S.; Krishnamoorti, R. Macromolecules 2000, 33, 3739.
24. Utracki, L. A. Clay-Containing Polymeric Nanocomposites, Vol. 2.; Rapra Technology Limited, Shrewsbury, UK, 2004.
25. Lee, K. M.; Han, C. D. Macromolecules 2003, 36, 804.
26. Krishnamoorti, R.; Giannelis, E. P. Macromolecules 1997, 30, 4097.
27. Nazockdast, E.; Nazockdast, H.; Goharpey, F. Polym Eng Sci 2008, 48, 1240.
28. Sinha Ray, S.; Okamoto, M. Prog Polym Sci 2003, 28, 1539.
29. Cervants-Uc, J. M.; Cauich-Rodrigues, J. V.; Vazquez-Torres, H.; Garfias-Mesias L. F.; Paul, D. R. Thermochim Acta 2007, 457, 92.